Thiosemicarbazones as Co-ordinating Agents. Solution Chemistry and *X*-Ray Structure of Pyridoxal Thiosemicarbazone Trihydrate and Spectroscopic Properties of its Metal Complexes†

M. Ferrari Belicchi, G. Fava Gasparri,* E. Leporati, C. Pelizzi, P. Tarasconi, and G. Tosi
Istituto di Chimica Generale ed Inorganica, Università di Parma, Centro di Studio per la Strutturistica Diffrattometrica del C.N.R., Via M.D'Azeglio 85, 43100 Parma, Italy

The ligand behaviour of pyridoxal thiosemicarbazone (H_2L) was examined in a series of metal complexes of formula $M(H_2L)X_2$, $M(HL)X$, and ML (M = Co, Ni, Cu, or Zn; X = NO_3 or CH_3CO_2) which were characterized by analytical methods and i.r. spectroscopy. Changes in the vibrational absorptions of the ligand upon co-ordination are discussed. The *X*-ray structure of uncomplexed $H_2L \cdot 3H_2O$ was determined. Crystals are monoclinic, space group $P2_1/n$, with $a = 16.126(1)$, $b = 7.267(1)$, $c = 12.466(1)$ Å, and $\beta = 108.60(1)°$. The structure was solved by direct methods and refined by full-matrix least squares to a final R value of 0.058 for 1 262 observed reflections. The thiosemicarbazone moiety shows an *E* configuration about both the C(2)–N(3) and C(1)–N(2) bonds, and the phenolic oxygen is *trans* to N(3). The protonation constants of H_2L were determined by spectrophotometric methods at 25 °C and $I = 0.5$ mol dm^{-3} (KCl): $\log \beta_{011} = 11.111(22)$, $\log \beta_{021} = 19.048(25)$, and $\log \beta_{031} = 23.342(27)$. The spectrophotometric characteristics of the various species are reported; the experimental spectra are in good agreement with calculated ones.

Transition-metal complexes of thiosemicarbazones are of great interest because of their chemical and pharmacological properties.[1–4] In a continuation of our studies on the chelating behaviour of N,S ligands towards transition metals such as iron, copper, zinc, and molybdenum,[5–7] the synthesis and structural investigation of metal complexes of thiosemicarbazones formed by organic substrates which have biological interest, such as pyruvic acid and pyridoxal derivatives, are now in progress. Combination of the pyridoxal moiety with a thiosemicarbazone system confers upon the final product interesting biological and chemical properties.

The present paper deals with the synthesis and the spectroscopic analysis of metal complexes with pyridoxal (3-hydroxy-5-hydroxymethyl-2-methylpyridine-4-carbaldehyde) thiosemicarbazone (H_2L), the synthesis and kinetic studies of which have recently been reported.[8] The metal complexes were prepared from acetates and nitrates of Co, Ni, Cu, and Zn. In order to gain more information about the structure and the ligand behaviour of the thiosemicarbazone, in solution and in the solid state, its *X*-ray structural analysis and u.v.–visible spectrophotometric characterization were also carried out.

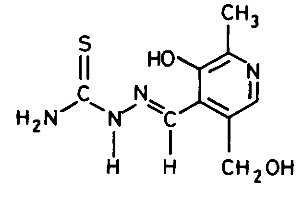

Experimental

Preparations.—Pyridoxal hydrochloride (Fluka) and thiosemicarbazide (Carlo Erba) were commercially available.

Pyridoxal, in its neutral form, and thiosemicarbazide (1:1 molar ratio) were dissolved in absolute ethanol and refluxed for about 2.30 h. After cooling a deep yellow microcrystalline product (m.p. 228 °C) was isolated [*m*/*z*:240 (53.8), 181 (13.8), 165 (100.0), and 60 (86.0%)]. The compound is soluble in warm ethanol and water, and scarcely soluble in chloroform.

An ethanol solution of the metal salt (acetate or nitrate) was added to an equimolar amount of pyridoxal thiosemicarbazone, dissolved in hot ethanol. The resulting solution was then heated for about 1 h and allowed to stand. When acetate was used a powder, the product, was obtained immediately. In the other cases, microcrystalline products were isolated after some days by slow evaporation of the solvent.

Physical Measurements.—Elemental C, H, N, and S analyses (Table 1) were carried out on a Perkin-Elmer model 240 automatic instrument. Metal analyses were done by atomic absorption spectroscopy on a Perkin-Elmer model 303 instrument. I.r. spectra were registered for KBr discs on a Perkin-Elmer model 283 B spectrophotometer, mass spectra on a Varian CH-5 spectrometer [70 eV (*ca.* 1.12×10^{-7} J)].

The pH measurements, using a Metrohm Titroprocessor E 636 equipped with a H268 glass electrode (Schott-Jena) and a B343 reference electrode Thalamide (Schott-Jena), were carried out as previously described[9] at 25 °C and $I = 0.5$ mol dm^{-3} (KCl). The electrode system was calibrated in terms of the standard electrode potential, E°, by performing strong acid *versus* strong base titrations and by calculation using the computer program NBAR.[10] U.v.–visible spectra were recorded on a Jasco spectrophotometer, model UVIDEC-505, equipped with a DP-101 digital printer. Matched quartz cells of pathlength 1.0 cm, calibrated before use, were employed. All the measurements were carried out at 25 °C and at an ionic strength I of 0.5 mol dm^{-3} (KCl). Absorption spectra were measured for 18 different aqueous solutions of H_2L in the range pH 2.562—12.219. For each solution, 49 absorbance data (H_2L, 230—470 nm), to the third decimal place, were collected on a digital printer with individual steps of 5.0 nm. All chemicals employed were of the highest grade available and were used as previously

---

† *Supplementary data available:* see Instructions for Authors, *J. Chem. Soc., Dalton Trans.*, 1986, Issue 1, pp. xvii—xx. Structure factors are available from the editorial office.

Table 1. Analytical data with calculated values in parentheses

Complex	Colour	Analysis/% C	H	N	S	M
$[Zn(H_2L)(NO_3)_2]\cdot H_2O$	Yellow-orange	24.0	3.3	19.1	6.9	15.0
		(24.2)	(3.2)	(18.8)	(7.2)	(14.6)
$[Co(HL)(NO_3)]\cdot 2H_2O$	Red-brown	26.9	4.1	18.0	8.4	15.5
		(27.3)	(3.8)	(17.7)	(8.1)	(14.9)
$[Ni(HL)(NO_3)]\cdot 2H_2O$	Red-orange	27.7	4.0	17.2	8.4	15.5
		(27.3)	(3.8)	(17.7)	(8.1)	(14.8)
$[Cu(HL)(NO_3)]\cdot 2H_2O$	Green	27.4	4.2	17.3	8.3	16.2
		(27.0)	(3.8)	(17.5)	(8.0)	(15.9)
$[Co(HL)(CH_3CO_2)]\cdot H_2O$	Brown	35.5	4.2	14.7	9.0	16.3
		(35.2)	(4.3)	(14.9)	(8.5)	(15.7)
$[Zn(HL)(CH_3CO_2)]\cdot H_2O$	Yellow-orange	35.2	4.1	14.5	9.0	17.5
		(34.6)	(4.2)	(14.7)	(8.4)	(17.1)
$[NiL]\cdot 2H_2O$	Red-brown	32.1	4.4	17.0	10.1	18.2
		(32.5)	(4.2)	(16.8)	(9.6)	(17.6)
$[CuL]\cdot 2H_2O$	Green	32.4	4.4	17.0	9.6	19.4
		(32.0)	(4.2)	(16.6)	(9.5)	(18.8)

Table 2. Initial concentrations (c_L/mol dm^{-3}), measured pH values and s.d.a.* of the solutions

10^4c_L	pH	s.d.a.	10^4c_L	pH	s.d.a.
0.573	3.807	9.072×10^{-3}	0.764	8.754	8.627×10^{-3}
0.764	11.678	9.804×10^{-3}	0.955	12.219	5.190×10^{-3}
1.223	4.896	1.080×10^{-2}	1.146	11.900	8.204×10^{-3}
1.146	9.359	8.871×10^{-3}	1.146	6.081	7.795×10^{-3}
1.146	5.882	7.168×10^{-3}	1.146	4.263	4.727×10^{-3}
1.146	5.121	9.879×10^{-3}	1.146	7.342	1.478×10^{-2}
1.146	10.002	7.644×10^{-3}	1.146	2.562	5.912×10^{-3}
1.146	10.617	1.055×10^{-2}	1.146	4.153	6.012×10^{-3}
1.146	4.711	7.054×10^{-3}	1.146	6.638	1.045×10^{-2}

* The standard deviation of the absorbance (s.d.a.) for each solution over all wavelengths is given by $\sum_{i=1}^{N}[A_c(i) - A_o(i)]^2/(N - N')$ where N is the number of wavelengths, $A_c(i)$ and $A_o(i)$ are the calculated and observed absorbances at point i, and N' is the number of protonation constants to be refined; $\beta_{pqr} = [M_pH_qL_r]/[M]^p[H]^q[L]^r$.

described.[11–14] Initial concentrations, pH values, and the standard deviation of absorbance after the refinement procedure (s.d.a.) for the aqueous solutions employed at the chosen ionic strength are reported in Table 2. The estimated errors in the measurements of pH and of absorbance were 0.002 and 0.005 units, respectively. A complete list of the experimental and theoretical absorbance data, as well as of the molar absorption coefficients, calculated by use of the program SQUAD, is available from the authors.

Crystallography.—Crystal data. $C_9H_{18}N_4O_5S$, $M = 294.3$, monoclinic, space group $P2_1/n$ (from systematic absences), $a = 16.126(1)$, $b = 7.267(1)$, $c = 12.466(1)$ Å, $\beta = 108.60(1)°$, $U = 1\,384.6(3)$ Å^3, $D_m = 1.43$ g cm^{-3}, $Z = 4$, $D_c = 1.41$ g cm^{-3}, $F(000) = 624$, $\lambda(\text{Cu-}K_\alpha) = 1.541\,78$ Å, $\mu(\text{Cu-}K_\alpha) = 22.6$ cm^{-1}, crystal size $0.07 \times 0.10 \times 0.33$ mm.

Intensity data and structure analysis. Intensity data were collected at room temperature on a Siemens AED single-crystal computer-controlled diffractometer by the ω—2θ scan technique ($5 < 2\theta < 120°$) with Cu-K_α radiation. The intensity of a standard reflection was measured every 20 reflections to check the stability of the crystal and the electronics. A total of 2 325 reflections were measured, of which only 1 271 having $I > 3\sigma(I)$ were considered observed and used in the subsequent analysis. No correction for absorption was applied.

Table 3. Fractional atomic co-ordinates ($\times 10^4$) for H_2L with estimated standard deviations in parentheses

Atom	*X/a*	*Y/b*	*Z/c*
S	−1 202(1)	−2(3)	8 593(1)
O(1)	−1 349(2)	2 907(7)	3 091(3)
O(2)	2 435(3)	2 457(8)	6 041(4)
O(3)	2 271(3)	1 330(8)	8 800(4)
O(4)	−2 543(4)	6 230(15)	9 503(6)
O(5)	−1 677(5)	4 423(9)	8 247(6)
N(1)	414(3)	731(9)	8 572(4)
N(2)	−704(3)	1 162(8)	6 902(4)
N(3)	−94(3)	1 731(8)	6 386(4)
N(4)	796(3)	3 897(8)	3 029(4)
C(1)	−436(4)	681(10)	8 003(5)
C(2)	−452(4)	2 085(10)	5 314(5)
C(3)	28(4)	2 681(9)	4 572(5)
C(4)	954(4)	2 829(9)	4 881(5)
C(5)	1 318(4)	3 448(10)	4 091(5)
C(6)	−78(4)	3 754(10)	2 675(5)
C(7)	−508(4)	3 088(10)	3 433(5)
C(8)	−569(4)	4 272(11)	1 472(5)
C(9)	1 553(4)	2 320(10)	6 053(5)

The structure was solved by direct methods and refined with initially isotropic and then anisotropic full-matrix least-squares cycles. All the hydrogen atoms were located from a Fourier difference synthesis, except H(23), H(15), and H(25) for which standard geometries were employed. A final blocked full-matrix least-squares cycle was computed including the H atoms not refined. The final R index was 0.058, $R' = 0.064$ using unit weights (observed reflections only). Nine reflections, which suffered errors during data reduction, were omitted in the last cycle. Scattering factors for all atoms were taken from ref. 15 and both the real and imaginary components of the anomalous dispersion were included. Final atomic co-ordinates for the non-hydrogen atoms are given in Table 3.

Calculations were made on the GOULD-SEL 77/22 computer of the Centro di Studio per la Strutturistica Diffrattometrica del C.N.R. (Parma), using the SHELX 76 program[16] for solution and refinement of the structure, PARST[17] for geometrical description of the structure, and PLUTO[18] and ORTEP[19] for the structure drawings.

Results and Discussion

Protonation Equilibria of H_2L.—The H_2L system has been investigated in detail by means of spectrophotometric methods

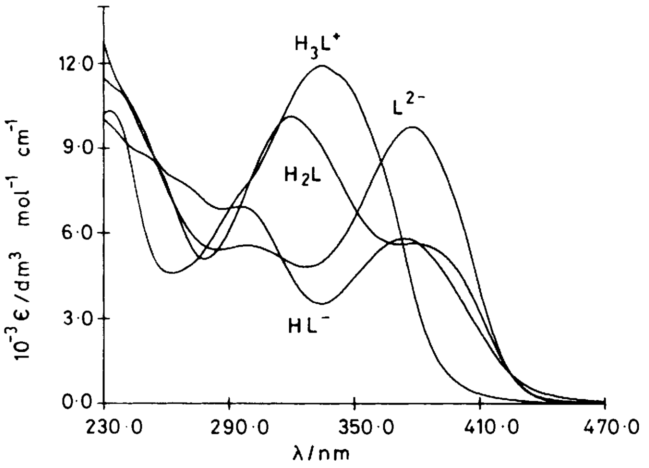

Figure 1. Calculated absorption spectra for four ionic forms of H_2L. These spectra together with the protonation constants were evaluated from spectra of 18 solutions in the range pH 2.562—12.219 using the computer program SQUAD with PLOTTER CALCOMP 936

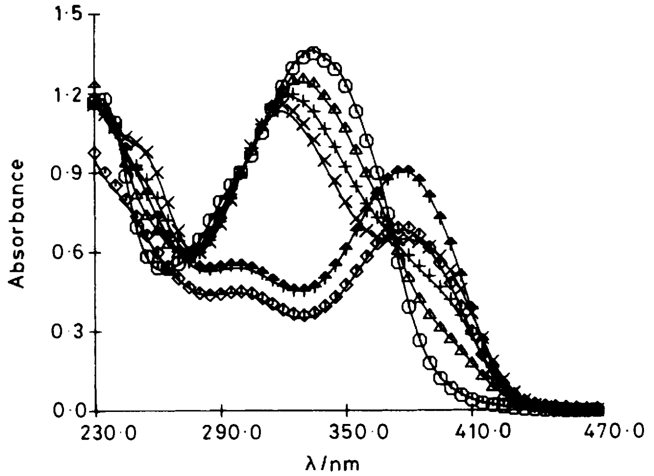

Figure 2. Comparison of some of the spectra used in calculating the curves in Figure 1 with theoretical curves constructed using the molar absorption coefficients from Figure 1 and the equilibrium constants by use of the program SQUAD. Calculated (full line) and experimental (symbols) absorption spectra for solutions of H_2L at pH 2.562 (○), 4.153 (△), 4.711 (+), 6.638 (×), 11.678 (◇), and 12.219 (▲)

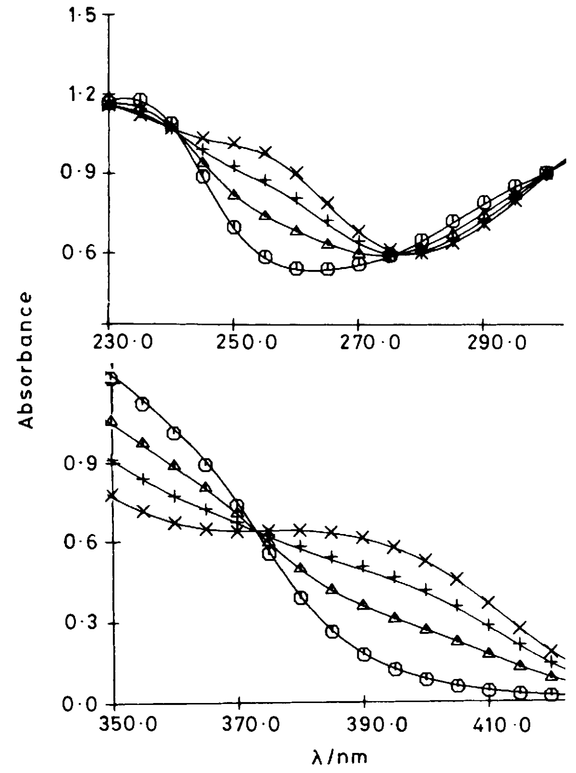

Figure 3. Isosbestic points obtained upon varying the pH for the ligand H_2L. See Figure 2 for meaning of symbols

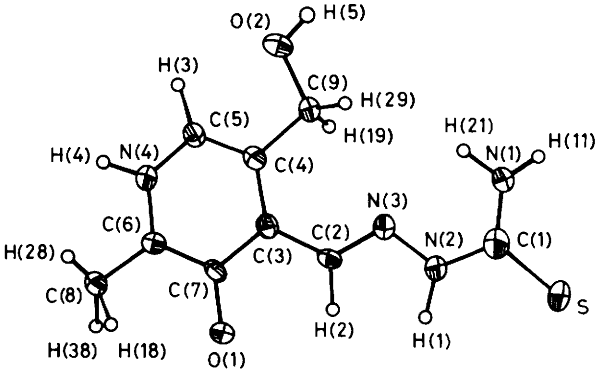

Figure 4. ORTEP drawing of the molecule of H_2L showing the atomic numbering scheme. Thermal ellipsoids enclose 50% probability and the hydrogen atoms were drawn with an arbitrary diameter

using the same calculation procedure used previously.[20–23] The protonation constants for H_2L have been obtained through the refinement of several sets of absorbance with the computer program SQUAD.[24] At 25 °C and $I = 0.5$ mol dm^{-3} (KCl) they are log $\beta_{011} = 11.111(22)$, log $\beta_{021} = 19.048(25)$, and log $\beta_{031} = 23.342(27)$. The protons can be assigned to the basic sites of the ligand on the basis of these results and by analogy with known values[25–27] for analogous functional groups: log $K_1^H = 11.111(22)$ and log $K_2^H = 7.937(24)$ can be probably assigned to the alcoholic (HL^-) and phenolic (H_2L) groups, respectively; while log $K_3^H = 4.294(26)$ can be ascribed to the protonation of the pyridine nitrogen atom (H_3L^+). However, it should be borne in mind that tautomeric forms (quinonoid and internal hemiacetal)[28–30] may exist for the species H_3L^+ and H_2L and that other pH-independent equilibria such as hydration to form carbinolamines may occur. Thus, the absorption spectra may contain contributions from such components when they are present. For Schiff bases of diamines, as with the present ligand, cyclic adducts may make major contributions to some ionic forms. For the most protonated form (H_3L^+) there is one major band at about 334 nm (Figure 1). The spectrum of the neutral form (H_2L) corresponding to the loss of the pyridine NH proton contains a peak at 319.8 nm.

For the HL^- form there must be one minor band, located at 374.0 nm. In alkaline solution the spectrum of the dianion (L^{2-}) has a maximum at 377.5 nm and possesses a higher molar absorption coefficient than does HL^-.

In acidic, neutral, and strongly basic media the absorption spectra (Figure 2) of H_2L show mainly two bands: a more intense peak at 319.8—334 nm and a weak band at 377.8 nm; moreover in strongly alkaline media the spectra show a weak broad peak which appears to be at a lower wavelength than 319.8 nm (*ca.*

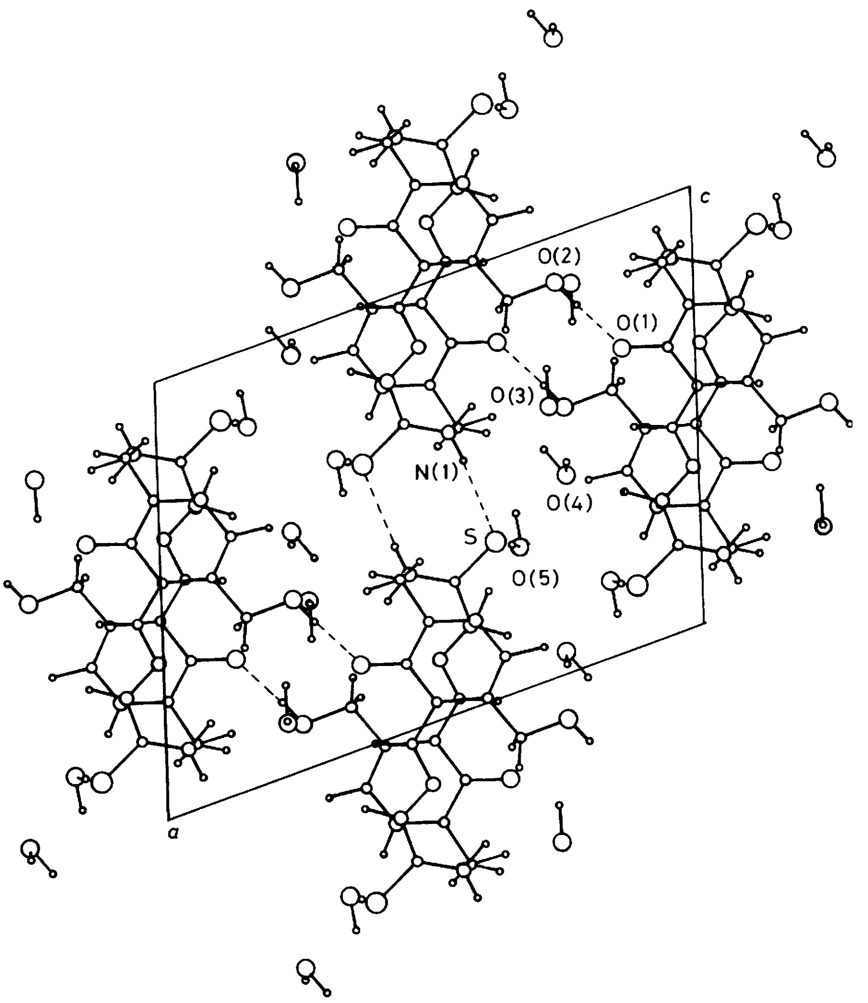

Figure 5. Projection of the structure along *b*

Table 4. Deviations (Å) of atoms from the planes and dihedral angle (°)

Plane (1) (pyridoxal ring): C(3), C(4), C(5), N(4), C(6), C(7)
[C(3) −0.020, C(4) 0.008, C(5) 0.009, N(4) −0.007, C(6) −0.005, C(7) 0.022, O(1) 0.054, C(8) −0.001, C(9) 0.040]

Plane (2) (thiosemicarbazone chain): N(1), C(1), S, N(2), N(3)
[N(1) 0.002, C(1) −0.007, S 0.000, N(2) 0.003, N(3) −0.001, C(2) 0.06]

Angle (1)—(2) 2.0

Table 5. Selected bond distances (Å) and angles (°)

S–C(1)	1.70(1)	C(4)–C(5)	1.37(1)
N(1)–C(1)	1.33(1)	N(4)–C(5)	1.36(1)
C(1)–N(2)	1.35(1)	N(4)–C(6)	1.34(1)
N(2)–N(3)	1.40(1)	C(6)–C(7)	1.42(1)
N(3)–C(2)	1.30(1)	C(6)–C(8)	1.50(1)
C(2)–C(3)	1.45(1)	C(4)–C(9)	1.52(1)
C(3)–C(4)	1.42(1)	O(1)–C(7)	1.29(1)
C(3)–C(7)	1.44(1)	O(2)–C(9)	1.43(1)
S–C(1)–N(1)	123.1(5)	N(2)–N(3)–C(2)	112.6(5)
S–C(1)–N(2)	118.4(5)	N(3)–C(2)–C(3)	124.2(6)
C(1)–N(2)–N(3)	120.1(5)		

300 nm). In acidic solutions the changes with pH involve a displacement of this unique band (334 nm) toward shorter wavelengths (319.8 nm, Figure 2). In particular, when the pH increases, small hypsochromic and hypochromic effects are observed from 334 to 319.8 nm. It may be concluded at this point that these absorption bands found in the near-u.v. and visible region arise from either $\pi \longrightarrow \pi^*$ or $n \longrightarrow \pi^*$ transitions. The only colour variation observed for H_2L is from pale yellow, in acidic solution, to a stronger yellow in strongly alkaline media. When the absorption spectra at various pH values (at constant ligand concentration) are compared, sharp isosbestic points are observed at 240.8, 276.6, and 373.0 nm (Figure 3). The presence of these points of constant absorption suggests that the simultaneous equilibria are altered by pH, and moreover indicate the coexistence of several species in solution. The refined molar absorption coefficients together with the calculated protonation constants were used to predict the spectra of the different solutions (Table 2) using the program SQUAD with PLOTTER CALCOMP 936. Comparison of observed and computed spectra, of which those in Figures 2 and 3 are typical, showed reasonable agreement.

Table 6. Hydrogen bond distances (Å) and angles (°)

Donor–hydrogen		Donor ··· acceptor		Hydrogen ··· acceptor		Donor–hydrogen ··· acceptor	
N(1)–H(11)	0.89	N(1) ··· S$^{\mathrm{I}}$	3.394(5)	H(11) ··· S$^{\mathrm{I}}$	2.57	N(1)–H(11) ··· S$^{\mathrm{I}}$	155
N(1)–H(21)	1.02	N(1) ··· N(3)	2.683(7)	H(21) ··· N(3)	2.28	N(1)–H(21) ··· N(3)	102
N(4)–H(4)	0.97	N(1) ··· O(3)	2.949(7)	H(21) ··· O(3)	2.20	N(1)–H(21) ··· O(3)	129
N(2)–H(1)	1.06	N(4) ··· O(5$^{\mathrm{II}}$)	2.735(10)	H(4) ··· O(5$^{\mathrm{II}}$)	1.79	N(4)–H(4) ··· O(5)	162
O(3)–H(13)	1.13	N(2) ··· O(4$^{\mathrm{III}}$)	2.811(7)	H(1) ··· O(4$^{\mathrm{III}}$)	1.76	N(2)–H(1) ··· O(4$^{\mathrm{III}}$)	180
O(3)–H(23)	1.12	O(3) ··· O(2$^{\mathrm{IV}}$)	2.851(8)	H(13) ··· O(2$^{\mathrm{IV}}$)	1.75	O(3)–H(13) ··· O(2$^{\mathrm{IV}}$)	162
O(4)–H(14)	1.17	O(3) ··· O(1$^{\mathrm{V}}$)	2.701(7)	H(23) ··· O(1$^{\mathrm{V}}$)	2.23	O(3)–H(23) ··· O(1$^{\mathrm{V}}$)	102
O(4)–H(24)	0.82	O(4) ··· O(3$^{\mathrm{VI}}$)	2.687(11)	H(14) ··· O(3$^{\mathrm{VI}}$)	1.66	O(4)–H(14) ··· O(3$^{\mathrm{VI}}$)	143
O(5)–H(15)	1.12	O(4) ··· O(2$^{\mathrm{VII}}$)	3.301(11)	H(24) ··· O(2$^{\mathrm{VII}}$)	2.51	O(4)–H(24) ··· O(2$^{\mathrm{VII}}$)	164
O(5)–H(25)	1.09	O(5) ··· S	3.302(7)	H(15) ··· S	2.19	O(5)–H(15) ··· S	178
O(2)–H(5)	0.87	O(5) ··· O(4)	2.742(12)	H(25) ··· O(4)	1.98	O(5)–H(25) ··· O(4)	124
		O(2) ··· O(1$^{\mathrm{V}}$)	2.692(5)	H(5) ··· O(1$^{\mathrm{V}}$)	1.83	O(2)–H(5) ··· O(1$^{\mathrm{V}}$)	174

Roman numeral superscripts refer to the following equivalent positions relative to the reference molecule at x, y, z: I $\bar{x}, \bar{y}, \bar{z} + 2$; II $\bar{x}, \bar{y} + 1, \bar{z} + 1$; III $\bar{x} - \frac{1}{2}, y - \frac{1}{2}, \bar{z} + \frac{3}{2}$; IV $\bar{x} + \frac{1}{2}, y - \frac{1}{2}, \bar{z} + \frac{3}{2}$; V $x + \frac{1}{2}, \bar{y} + \frac{1}{2}, z + \frac{1}{2}$; VI $\bar{x}, \bar{y} + 1, \bar{z} + 2$; VII $x - \frac{1}{2}, \bar{y} + \frac{1}{2}, z + \frac{1}{2}$.

Table 7. Selected vibrational bands (cm^{-1}) of H_2L and the complexes of Co, Ni, Cu, and Zn

	$\nu(NH_2)$, $\nu(OH)$	$\nu(NH)$	$\nu(NH^+)$, $\nu(OH)$	$\nu(C=N)$, $\nu(C=C)$	Ring	$\nu(C=N)$	Ring	δ(OH)	δ(NCS)	$\nu(C=S)$	δ(CH)
H_2L	3 390m, 3 250m	3 160m	2 860(sh)	1 600s	1 570mw	1 540s	1 505(sh), 1 498s, 1 465m, 1 430m, 1 415m	1 375vs	1 250s, 1 220m, 1 090s, 1 035vs	920m	825ms, 815(sh)
$[Zn(H_2L)(NO_3)_2]\cdot H_2O$	3 460(sh), 3 300m, 3 240m	3 150m	2 870w	1 620s, 1 600(sh)	1 575(sh)	1 560s	1 500s, 1 460(sh), 1 440(sh), 1 410(sh)	1 385vs	1 250m, 1 215ms, 1 150m, 1 015ms	840mw	825m
$[Co(HL)(NO_3)]\cdot 2H_2O$	3 500(sh), 3 260m, 3 180m	—	2 880w, 2 700w	1 640(sh), 1 620(sh), 1 600ms	1 570m	1 560(sh)	1 490ms, 1 460s, 1 440s	1 385vs	1 250m, 1 210m, 1 150m, br, 1 090mw, 1 020mw	900w, 835(sh)	825m
$[Ni(HL)(NO_3)]\cdot 2H_2O$	3 500m, 3 350m	—	2 600m	1 660(sh), 1 620ms	1 575m, br	—	1 500s, 1 460m, 1 430(sh)	1 385vs	1 245m, 1 210m, 1 170m, 1 005m	855mw	825m
$[Cu(HL)(NO_3)]\cdot 2H_2O$	3 485m, 3 475(sh), 3 400(sh), 3 360s, 3 310(sh)	—	2 750m, 2 690(sh)	1 630m, 1 605w	1 585s	1 565s	1 500s	1 385vs	1 250m, 1 215ms, 1 150m, 1 015ms	860m, 840m	825m
$[Co(HL)(CH_3CO_2)]\cdot H_2O$	3 620m, 3 430br, 3 300m, br, 3 180m	—	2 850w	1 610(sh)	1 575vs	1 540vs	1 500(sh), 1 450s	1 380s	1 260w, 1 200w, 1 150m, 1 030s	930m	800m, br
$[Zn(HL)(CH_3CO_2)]\cdot H_2O$	3 480m, 3 390m, br, 3 240m	—	2 900w	1 620s, br	1 575m	—	1 515mw, 1 490(sh), 1 460(sh), 1 410s	1 380m	1 270ms, 1 200m, 1 140ms, 1 020mw	880(sh), 875m	800m
$[NiL]\cdot 2H_2O$	3 440m, br, 3 320ms, 3 190m	—	—	1 600s	1 570m	—	1 505(sh), 1 495vs, 1 425s	1 375ms	1 260ms, 1 190ms, 1 150m, 1 015ms	860w	815w
$[CuL]\cdot 2H_2O$	3 440(sh), 3 340m, 3 290m	—	—	1 625m, br, 1 600s, br	1 580(sh)	—	1 505(sh), 1 490vs, 1 470(sh), 1 415s	1 370m	1 270m, 1 195ms, 1 165(sh), 1 025m	870w	800w

Description of the Structure.—The structure consists of molecules of pyridoxal thiosemicarbazone and water. Figure 4 shows an ORTEP drawing of the molecule and Figure 5 a projection of the structure on the (010) plane. The pyridoxal ring adopts the role of a zwitterion where the nitrogen atom is protonated and the phenolic oxygen is deprotonated, as previously observed for other pyridoxal-containing derivatives.[31,32]

The whole system is almost planar (Table 4). The pyridine ring is planar within experimental error and is twisted by only 2°36′ with respect to the side chain. Similar behaviour was observed for 5-hydroxypyridine-2-carbaldehyde thiosemicarbazone,[33] and 4-phenylpyridine-2-carbaldehyde thiosemicarbazone[34] but it is in contrast with the structure of pyridine-4-carbaldehyde thiosemicarbazone[35] in which the side chain is twisted by 14° with respect to the plane of the pyridine ring.

The thiosemicarbazone moiety shows an *E* configuration both about C(2)–N(3) and C(1)–N(2). The phenolic oxygen is *trans* to N(3). A comparison of the bond distances in the side chain (Table 5) with those previously reported for other thiosemicarbazone structures[33–37] reveals a higher delocalization of the system. However, small differences in bond lengths may be perturbed by the different hydrogen-bonding patterns, important in all thiosemicarbazones. The water molecules, and the OH and CH_2OH groups, are involved in an extensive hydrogen-bonding network as illustrated in Figure 5 and in Table 6. There are dimer-like molecules (similar to those found in other thiosemicarbazones) formed by N–H $\cdots$ S hydrogen bonds across a centre of symmetry.

Bond distances and angles in the pyridoxal ring (Table 5) are in agreement with those found in other compounds containing the same moiety[30,31] when a zwitterion is adopted. The C(5)–N(4)–C(6) angle of the pyridine ring [124.1°(5)] is significantly greater than 120° and is characteristic for a protonated nitrogen. This is also in agreement with the N(4) $\cdots$ O(5) distance [2.74(1) Å] corresponding fairly well to a hydrogen bond and with the O(1)–C(7) distance [1.29(1) Å] which is intermediate between a single (1.43 Å) and double bond (1.23 Å).

The packing is characterized by sheets formed by water molecules and organic dimers which are alternately disposed along the *Z* axis. Atom H(21) is weakly intermolecularly hydrogen bonded to O(3) and intramolecularly bonded to N(3) (Table 6) to form a three-centre ('bifurcated') hydrogen bond.

The conformation of the compound places N(1) *cis* to N(3) and in the best orientation for intramolecular hydrogen bonding to N(3). The molecule rotated 180° about C(1)–N(2) and also 180° about C(2)–C(3), with the ONS functional groups placed on the same side, could act as a tridentate ligand, such as is hypothesized to have cytotoxic activity.[38]

Metal Complexes.—In all the compounds the metal:ligand molar ratio is 1:1, even though three types of stoicheiometries are exhibited, $M(H_2L)X_2$, M(HL)X, and ML, as a consequence of the nature of the inorganic anion and of the different form (neutral, mono-, or di-deprotonated) that the ligand assumes. It is worthy of note that H_2L acts as a di- or mono-deprotonated ligand when it reacts with metal acetates, and as neutral or monodeprotonated when metal nitrates are used.

The main vibrational bands of H_2L and its metal complexes are reported in Table 7. An interesting feature of the spectra concerns the differences, mainly as a result of the different stoicheiometries of the metal complexes. While a similar spectroscopic pattern is shown by $[NiL]\cdot 2H_2O$ and $[CuL]\cdot 2H_2O$, $[Co(HL)(CH_3CO_2)]\cdot H_2O$ and $[Zn(HL)(CH_3CO_2]\cdot H_2O$ exhibit some significant differences which are probably caused by the uni- or bi-dentate ligand behaviour of the co-ordinated acetate group. The complex $[Zn(H_2L)(NO_3)_2]\cdot H_2O$ shows an i.r. spectrum which differs from those of all the other complexes, while the derivatives of Co, Ni, and Cu, which all contain the monodeprotonated ligand, exhibit some differences which can be again explained by the different ligand behaviour of the nitrate group.

An accurate interpretation of the i.r. spectra is therefore made difficult by these differences as well as by the absorptions due to the pyridoxal moiety; nevertheless some general conclusions can be made. For all the complexes the stretching vibrations of the NH_2 and OH (water and hydroxymethyl) groups appear in the 3 500—3 400 cm^{-1} region, the absorption of the NH group occuring at lower wavenumbers (*ca.* 3 200 cm^{-1}); this last band disappears when deprotonation occurs.[39] The absorptions which are observed below 3 000 cm^{-1} can be attributed to the NH^+ group of the pyridine ring, whose protonation is a consequence of the migration of the hydrogen atom from the phenolic OH to the pyridine nitrogen.[32,40,41] No bands are observed at 2 500 cm^{-1} assignable to the SH group.

The assignment of bands involving the C=S group is often uncertain and difficult owing to the large range (1 300—700 cm^{-1}) in which the ν(C=S) band is generally found.[39,42–46] In our opinion this mode can be correctly attributed to the band at *ca.* 920 cm^{-1} in the free-ligand spectrum, even if the bands observed at *ca.* 1 250, 1 030, and 770 cm^{-1} also contribute to the C=S stretching mode. The shift (20—50 cm^{-1}) in this band for the metal complexes indicates involvement of the sulphur atom in bonding to the metal. Some complexes show absorptions in the 450—300 cm^{-1} range which could be attributed to the ν(M–S) vibration,[1,47] *i.e.* $[Cu(HL)(NO_3)]\cdot 2H_2O$ (420m and 328mw) and $[Co(HL)(CH_3CO_2)]\cdot H_2O$ (415m and 320mw cm^{-1}), but the assignments are uncertain in all these cases.

On the basis of the shifts observed for the C=N groups it can be deduced that the imine nitrogen atom seems to be involved in co-ordination to the metal atom. The participation of the phenolic oxygen in co-ordination is not clear even though a comparison with spectroscopic data previously reported for metal complexes of pyridoxal acylhydrazones suggests that in this case also the oxygen atom could be involved in co-ordination.[32,48]

As regards the inorganic anion, in $[Zn(H_2L)(NO_3)_2]\cdot H_2O$ [$\nu(NO_3)$ 1 385 cm^{-1}] the nitrate group shows ionic character, while in the cobalt, nickel, and copper complexes it is covalently bonded; in particular, this ligand seems to be unidentate in $[Co(HL)(NO_3)]\cdot 2H_2O$ [$\nu_{asym}(NO_3)$ 1 465, $\nu_{sym}(NO_3)$ 1 335 cm^{-1}] and bidentate in $[Cu(HL)(NO_3)]\cdot 2H_2O$ [$\nu_{asym}(NO_3)$ 1 565, $\nu_{sym}(NO_3)$ 1 340 cm^{-1}] and in $[Ni(HL)(NO_3)]\cdot 2H_2O$ [$\nu_{asym}(NO_3)$ 1 510, $\nu_{sym}(NO_3)$ 1 320 cm^{-1}].[49,50] The acetate group is probably unidentate in $[Co(HL)(CH_3CO_2)]\cdot H_2O$ [$\nu_{asym}(CH_3CO_2)$ 1 540, $\nu_{sym}(CH_3CO_2)$ 1 410 cm^{-1}] and bidentate in $[Zn(HL)(CH_3CO_2)]\cdot H_2O$ [$\nu_{asym}(CH_3CO_2)$ 1 590, $\nu_{sym}(CH_3CO_2)$ 1 410 cm^{-1}].[51]

In conclusion, the analytical and spectroscopic data suggest probably ONS terdentate ligand behaviour for the thiosemicarbazone, as can be deduced from a preliminary *X*-ray analysis carried out on the $[Mn(H_2L)Cl_2]\cdot H_2O$ complex.[52] At present, *X*-ray structural analyses and spectroscopic studies on metal complexes of pyridoxal and pyruvic acid thiosemicarbazones are in progress in our laboratory. Moreover, in order to obtain a fuller understanding of the influence exerted by the thiosemicarbazone geometry on its co-ordinating and antitumour properties, our work will be also extended to the bisthiosemicarbazones of aromatic and heteroaromatic dialdehydes or diketones.

References

1 S. Padhyé and G. B. Kauffman, *Coord. Chem. Rev.*, 1985, **63**, 127.
2 V. M. Leovac, V. Divjakovic, D. Petrovic, G. Argay, and A. Kalman, *Polyhedron*, 1983, **2**, 1307.
3 M. P. Martinez, M. Valcarcel, and F. Pino, *Anal. Chim. Acta*, 1976, **81**, 157.
4 G. W. Bushnell and A. Y. M. Tsang, *Can. J. Chem.*, 1979, **57**, 603.
5 M. Belicchi Ferrari, G. Fava Gasparri, and C. Pelizzi, *Inorg. Chim. Acta*, 1981, **55**, 167.
6 C. Lorenzini, C. Pelizzi, G. Pelizzi, and G. Predieri, *J. Chem. Soc., Dalton Trans.*, 1983, 2155.
7 M. Belicchi Ferrari, G. Fava Gasparri, C. Pelizzi, and P. Tarasconi, *Inorg. Chim. Acta*, 1985, **97**, 99.
8 L. Ballesteros and D. Perez-Bendito, *Analyst (London)*, 1983, **108**, 443.
9 E. Leporati, *Anal. Chim. Acta*, 1985, **170**, 287.
10 H. S. Harris and R. S. Tobias, *Inorg. Chem.*, 1969, **8**, 2259.
11 F. Bigoli, E. Leporati, and M. A. Pellinghelli, *J. Chem. Soc., Dalton Trans.*, 1981, 1961.
12 F. Bigoli, E. Leporati, and M. A. Pellinghelli, *J. Chem. Soc., Dalton Trans.*, 1981, 1531.

13 A. Braibanti, F. Dallavalle, E. Leporati, and G. Mori, *J. Chem. Soc., Dalton Trans.*, 1973, 2539.
14 E. Leporati, *J. Chem. Soc., Dalton Trans.*, in the press.
15 'International Tables for *X*-Ray Crystallography,' Kynoch Press, Birmingham, 1974, vol. 4.
16 G. M. Sheldrick, SHELX 76, A Program for Crystal Structure Determination, University of Cambridge, 1976.
17 M. Nardelli, *Comput. Chem.*, 1983, **7**, 95.
18 W. D. S. Motherwell, PLUTO, University of Cambridge, 1976.
19 C. K. Johnson, ORTEP, Report ORNL-3794, Oak Ridge National Laboratory, Tennessee, 1965.
20 M. Biagini Cingi, F. Bigoli, E. Leporati, and M. A. Pellinghelli, *J. Chem. Soc., Dalton Trans.*, 1982, 1411.
21 M. Biagini Cingi, F. Bigoli, E. Leporati, and M. A. Pellinghelli, *J. Chem. Soc., Dalton Trans.*, 1982, 1965.
22 E. Leporati, *Ann. Chim. (Rome)*, 1983, **73**, 1.
23 F. Bigoli, E. Leporati, and M. A. Pellinghelli, *Ann. Chim. (Rome)*, 1983, **73**, 481.
24 D. J. Leggett and W. A. E. McBryde, *Anal. Chem.*, 1975, **47**, 1065.
25 K. Nagano and D. E. Metzler, *J. Am. Chem. Soc.*, 1967, **89**, 2891.
26 J. T. Wrobleski and G. J. Long, *Inorg. Chem.*, 1977, **16**, 2752.
27 R. M. Motekaitis and A. E. Martell, *Can. J. Chem.*, 1982, **60**, 2403.
28 C. M. Metzler, A. Cahill, and D. E. Metzler, *J. Am. Chem. Soc.*, 1980, **102**, 6075.
29 D. Heinert and A. E. Martell, *J. Am. Chem. Soc.*, 1963, **85**, 188.
30 D. Heinert and A. E. Martell, *J. Am. Chem. Soc.*, 1959, **81**, 3933.
31 P. Domiano, A. Musatti, M. Nardelli, C. Pelizzi, and G. Predieri, *Inorg. Chim. Acta*, 1980, **38**, 9.
32 P. Domiano, A. Musatti, M. Nardelli, C. Pelizzi, and G. Predieri, *Transition Met. Chem.*, 1979, **4**, 351.
33 G. J. Palenik, D. F. Rendle, and W. S. Carter, *Acta Crystallogr., Sect. B*, 1974, **30**, 2390.
34 J. N. Brown and K. C. Agrawal, *Acta Crystallogr., Sect. B*, 1977, **33**, 980.
35 R. Restivo and G. J. Palenik, *Acta Crystallogr., Sect. B*, 1970, **26**, 1397.
36 J. N. Brown and K. C. Agrawal, *Acta Crystallogr., Sect. B*, 1978, **34**, 2038.
37 J. N. Brown and K. C. Agrawal, *Acta Crystallogr., Sect. B*, 1978, **34**, 1002.
38 W. Antholine, J. Knight, H. Whelan, and D. H. Petering, *Mol. Pharm.*, 1977, **13**, 89.
39 M. F. Iskander and L. El-Sayed, *J. Inorg. Nucl. Chem.*, 1971, **33**, 4253.
40 S. P. Mital, R. V. Singh, and J. P. Tandon, *J. Inorg. Nucl. Chem.*, 1981, **43**, 3187.
41 Y. Matsushima, *Chem. Pharm. Bull.*, 1968, **16**, 2143.
42 R. K. Sharma, R. V. Singh, and J. P. Tandon, *J. Inorg. Nucl. Chem.*, 1980, **42**, 463.
43 D. M. Wiles and T. Suprunchuk, *Can. J. Chem.*, 1968, **46**, 1865.
44 M. A. Ali, S. E. Livingstone, and D. J. Phillips, *Inorg. Chim. Acta*, 1973, **7**, 531.
45 Anil Saxena and J. P. Tandon, *Polyhedron*, 1984, **3**, 681.
46 K. A. Jenesen and P. H. Nielsen, *Acta Chem. Scand.*, 1966, **20**, 597.
47 S. E. Livingstone and J. E. Oluka, *Transition Met. Chem.*, 1977, **2**, 163.
48 M. Nardelli, C. Pelizzi, and G. Predieri, *Transition Met. Chem.*, 1978, **3**, 233.
49 N. F. Curtis and Y. M. Curtis, *Inorg. Chem.*, 1965, **4**, 804.
50 A. B. P. Lever, E. Mantovani, and B. S. Ramaswamy, *Can. J. Chem.*, 1971, **49**, 1957.
51 K. Nakamoto, J. Fujita, S. Tanaka, and M. Kobayashi, *J. Am. Chem. Soc.*, 1957, **79**, 4904.
52 M. Belicchi Ferrari, G. Fava Gasparri, C. Pelizzi, P. Tarasconi, and G. Tosi, *Rev. Port. Quim.*, 1985, **27**, 328.

Received 6th *January* 1986; *Paper* 6/031